Applied Nanoscience (2020) 10:3577–3584
https://doi.org/10.1007/s13204-020-01459-y

ORIGINAL ARTICLE

Thuja occidentalis mediated AuNPs as wound dressing agents for abdominal wound healing in nursing care after surgery

Yan Dong[1] · Xiu-Mei Hu[1] · Yun-Feng Cao[1] · Ya-Chao Wang[1] · Ling-Zi Li[1] · Jian-Yu Lu[1] · Xiu-Xia Li[1]

Received: 18 March 2020 / Accepted: 20 May 2020 / Published online: 10 June 2020
© King Abdulaziz City for Science and Technology 2020

Abstract
Prevention of infection at the surgical area and outbreak of wounds are the most important and at the same time challenging tasks in clinical care. This research investigates the healing effect of laparotomy wounds after the use of bio-fabricated gold nanoparticles (Au NPs) prepared utilizing *Thuja occidentalis* leaf extract. Ultraviolet–visible (UV–Vis) spectroscopy and X-ray diffraction (X-RD) results confirmed the successful formation of Au NPs. High-resolution Transmission Electron Microscopy (HR-TEM) images confirmed the formation of spherical shaped Au NPs comprising of 30–50 nm particle size. Dermal fibroblasts were subjected to increased concentrations of Au NPs and their effect of cytotoxicity and synthesis of collagen was evaluated. The procedure of celiotomy was conducted on rabbits where the surgical area was exposed topically with either vehicle or once/everyday with Au NPs for about 14 days. Au NPs raised the collagen production from dermal fibroblasts and improved the expression of caspase 3 by exposure to a long period. AuNPs also showed cytotoxic impact with half-maximal inhibitory concentration (IC_{50}) of 0.16 mg/mL. Regular treatment of surgical area with AuNPs led to higher collagen deposition with reduced microbial load and enhanced healing of wounds.

Keywords Au NPs · Abdominal wound healing · Fibroblasts

Introduction

Laparotomy is recognized as one among the commonly conducted surgical procedures in medical care. Infection in surgical area as well as wound dehiscence are the important complications of post laparotomy surgery. The incidence rate of infection at the surgical site ranges from 2.5 to 41.9% globally (Mawalla et al. 2011). The possibility of occurring wound dehiscence after laparotomy surgery ranges from 0.25 to 3%, (Hugh 1990; Mokela et al. 1995; Heller et al. 2006) however, such cases sometimes require emergency surgery that often results in fatal and 20% of these patients have reported being dead (Spiliotis et al. 2009). Like many other causes including hematoma, improper usage of the procedure, and suture material, infection at the operational site is also a prominent cause of wound dehiscence post laparotomy. Laparotomy includes making a complete thickness injury in the abdomen, which involves the peritoneum to enter the abdominal cavity, rendering the wound more vulnerable to systemic and local infections relative to superficial wounds; in turn, the existence of fat in the abdomen could be an added factor to increased risks of post-laparotomy infection. It is therefore important to make sure of the early restoration of wound strength to avoid dehiscence of the wound which may cause evisceration. In this regard, prevention of postoperative microbial load and initiating early restoration of wound strength to ensure successful post-surgical rehabilitation would be worthwhile.

Antibiotic resistance during the treatment of infection is one of the major challenges for physicians and surgeons. Metal NPs exhibit remarkable antimicrobial activity without any report of microbial resistance and they also display enhanced collagen deposition (Kwan et al. 2011). Therefore, owing to these qualities, metal NPs are helpful for laparotomy wound healing. Thus, the present research was intended to assess the effect of Au NPs on post-laparotomy wound healing for the first time, even though similar research was recently reported in medical practice to utilize metals as antibacterial agents in wound healing after laparotomy (Arhi and El-Gaddal 2013). The increasing interest in utilizing Au

✉ Xiu-Xia Li
XiuXiaLi12@outlook.com

[1] Department of General Surgery, Weifang People's Hospital, No. 151 Guangwen Street, Kuiwen District, Weifang, Shandong 261041, China

NPs has raised concerns about the safety of Au NPs along with their judicious applications. The effective antimicrobial action of metals is considerably enhanced on decreasing its size (Pal et al. 2007), however, the toxicity of Au has increased (Liu et al. 2010; Koohi et al. 2011). Hence it is very necessary to maintain a balance between its toxicity and potential therapeutic benefit by choosing the optimal size of nanoparticles. On the other hand, the increased costs of antibiotic production and the improved microbial resistance to antibiotics, the green production of NPs involving less energy consumption, and economical feasibility is an attractive proposition. Subsequently, plant extract mediated approaches involving the use of plant antioxidants have been established to generate low cost and eco-friendly NPs. Further, the increased resistance of these disease-causing microbes to antibiotic drugs and biofilms formation, development of new antimicrobials with less cost is of higher demand and the effort to develop clinical antibacterial agents is increasing quickly. Due to the necessity of managing with drug-resistant pathogens, the present work showed the biosynthesis of Au NPs which were typically used on the wounds of laparotomy to determine their effectiveness in decreasing microbial load, enhancing the healing of the wound and detecting systemic side effects.

The current research demonstrates the fabrication of Au NPs using leaf extract of *Thuja occidentalis.* Then, the dermal fibroblasts were subjected to increased concentrations of Au NPs and their effect on cytotoxicity and collagen production was evaluated. Laparotomy procedure was done on rabbits and the surgical area was exposed topically either with a vehicle once/everyday with Au NPs for 14 days to check the wound healing efficiency of prepared Au NPs.

Materials and methods

Fabrication and characterization of Au NPs using Thuja occidentalis extract

Thuja occidentalis plant extract was used to synthesize Au NPs. Briefly, the suitable amount of extract was taken and stirred along with double distilled (DD) water, followed by the addition of $HAuCl_4$ solution (4 mM) drop by drop to make 20 ml of the final volume. Later, the resultant mixture was subjected to incubation overnight at 25 °C and the formation of Au NPs was evaluated with the help of a UV–Vis spectrophotometer operated at an average wavelength ranging from 200 to 1000 nm. The dilution quantity of *Thuja occidentalis* extract is used as a control blank solution.

The following analyses were performed after the fabrication of Au NPs from Thuja occidentalis plant extract to confirm the formation of Au NPs. The crystallite morphology of dried NPs was characterized with the help of XRD analysis. The morphological properties of formed Au NPs were observed through TEM and Selected Area Electron Diffraction (SAED) images. The existence of elemental Au in the fabricated Au NPs was examined with the help of Energy Dispersive X-Ray Spectroscopy (EDXS) analysis. The analysis of Fourier-Transform Infrared Spectroscopy (FTIR) was utilized to examine the formed Au NPs and their functional biomolecules by measuring FTIR spectrum of dried Au NPs, at a wavelength ranging from 400 to 4000 cm^{-1}.

Cell culture

Sprague–Dawley (female) rats weighing 100 g approximately were surrendered using ketamine HCL and Xylazine anesthesia in excess quantity. A minor portion of the skin was excised after hair removal, further small explants were cultured using DMEM medium consisting of 10% FBS at 37 °C in T_{25} tissue culturing flasks with 5% CO_2. The skin fibroblasts were slowly divided and transferred to develop confluent monolayer inside 2–3 weeks. Cells were eventually sub-cultured for future purposes inside T_{25} culture flasks.

Immunocytochemistry

The skin fibroblasts are subjected to culture on the coverslips for about a day. Then, the cells were left treated/untreated in serum-deprived medium with specific doses of Au NPs followed by incubation for 2 days. Furthermore, coverslips were cleaned utilizing Hanks' Balanced Salt Solution (HBSS) thrice; then the cells were fixed in 4% paraformaldehyde for a period of 20 min and then washed with phosphate-buffered saline(PBS) solution followed by permeabilizing for 1 min on ice utilizing 0.1% Triton X-100. Furthermore, at ambient temperature, the cells were covered with 3% goat serum for 60 min and cleaned using PBS-T (triton-X of 0.03%) and kept in an incubator with antibody, anti-collagen I (1:100, Abcam, 34,710) for the whole night in a humid chamber at 4 °C. The cells were incubated for about 2 h at ambient temperature along with secondary antibody (Alexa Fluor 488 goat anti-rabbit IgG, Invitrogen, A11034) after being washed with PBS-T. Later, the Cells were rinsed thrice using PBS and the nuclei were stained utilizing DAPI for analyzing under a fluorescence microscope.

MTT assay

The skin fibroblasts viability after exposure to various doses of Au NPs was tested by MTT assay following test protocol utilizing assay kit (Millipore, MA, USA). In brief, skin fibroblast cells of density 10^4 were added into each well of 96-well plates and grown throughout the night. The as-prepared Au NPs at a particular concentration was added to the culturing media and were pipetted followed by transferring

to each well and then subjected for incubation. The culture was substituted by MTT after 96 h and incubated again at 37 °C. Formazan crystals were solubilized after 3 h with isopropanol solution and were then analyzed utilizing an enzyme-linked immune sorbent assay (ELISA) reader, later the absorbance was calculated at a wavelength of 595 nm along with 600 nm as a reference wavelength.

Animal studies

The study was conducted with the approval from Institutional Animal Ethical Committee (approval number: W1020120190301S) and all the experiments were performed according to their guidelines. The study was performed using 12 healthy white female rabbits (30 mg/kg) with similar body weights and about one year old.

Experiment

Ketamine hydrochloride of 30 mg/kg and Xylazine hydrochloride of 6 mg/kg was utilized to anesthetize the animals. The abdomen was made ready for laparotomy surgical treatment, furthermore, the hair of the animals was removed utilizing chemical epilation, and then betadine solution was utilized to cautiously disinfect the surgical area. Then, a sterile drape was used to cover the abdominal area. Furthermore, an incision of 4 cm was made alongside the linea alba in the skin which is the rectus abdominis sheath. Subcutaneous connective tissue was sharply dissected using a pair of scissors to see the linea alba, further occasional swabbing for hemostasis was performed. By tenting the linea alba, the abdomen was entered followed by stab incision, then incision made was extended with the help of scissors. Simple interrupted sutures were made to close the muscular layers with the help of catgut (2–0), which is accompanied by sub-cuticular sutures for covering the pocket. Suturing of skin was done with silk then the final region of the surgical site was measured as 12 cm^2. After laparotomy surgery, 12 animals were blindly divided into three different groups as follows, for about 2 weeks at the surgical site over the incision line. The site of injury was covered with the help of soft bandage in all the animals and changed regularly after dressing. Except for Au NPs and PBS, no other systemic or local treatment was implemented.

Group I (Control): Treatment with 1 mL PBS topically applied to the operation site along the line of incision.

Group II: Single treatment of AuNPs (10 mg/1 mL of PBS) topically applied to the operation site along the line of incision.

Group III: Daily treatment of AuNPs (10 mg/1 mL of PBS) topically applied to the operation site along the line of incision for 14 days.

Histological studies

All the rabbits were euthanized using a barbiturate overdose at the end of the 14-day study period. The tissue samples from the heart of the incision sites were collected for histopathology in 10% formalin. Tissues fixed in formalin are cleaned in xylene followed by dehydrating using graded ethanol and finally subjected in paraffin. Microtome was utilized to prepare 5-micron sections and Sirius red was utilized to stain few portions of the skin in the incision site.

Bacterial count

Sterile swabs were obtained from all 12 rabbits on 7th day after surgery for bacterial load assessment. The cotton swab was scrubbed mildly onto the skin of separate incision lines with attention to avoid contact with accompanying tissues and placed in a sterilized vial. Swab obtained from each surgical region was dissipated in sterile PBS (with pH 7.4) solution and was diluted ten folds using the same PBS solution. From a higher dilution (about 6–10), a sample of 10 µL was spread over the Nutrient Agar media for each swab followed by incubating overnight at a temperature of 37 °C. The number of bacterial colonies was calculated on the next day and microbial load was presented as the colony-forming unit (cfu). The amount of microbial load at the surgical region was measured as an average microbial load percentage (%) of animals inside PBS and the percentage difference in bacterial load was represented as average ± SD.

Results and discussion

Initially, the development of bio-fabricated Au NPs was confirmed by the absorbance value of NPs with the help of UV–Vis spectroscopy. According to the results obtained from past studies, bio-fabricated Au NPs have familiar précised peak values in between 540 and 560 nm (Geetha et al. 2013; Chueh et al. 2014). The fabrication of Au NPs was evident by the change in solution color to ruby-red from mild-yellow and also by the existence of standard plasmon band ranging in between 525 and 540 nm with a maximum absorbance peak noticed in between 535 to 527 nm. The distinct characteristics of the standard plasmonic peak demonstrated the oval and spherical shape of Au NPs with length ranging from 30 to 50 nm. The reaction was observed in reaction kinetics of UV–visible spectroscopy studies after 24 h–30 days as displayed by the plasmonic peak stability (Fig. 1). Beer-Lambert's law was utilized to analyze the concentration of Au NPs spectrophotometrically with an extinction coefficient of $\varepsilon = 1.8 \times 1010\ M^{-1}\ cm^{-1}$ for a 50 nm particle diameter. Anisotropic Au NPs were reported to display two excellent

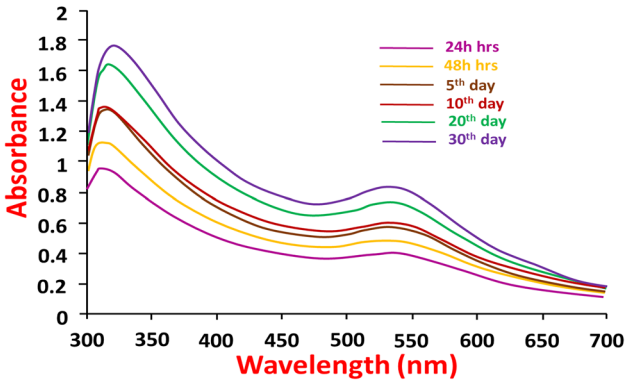

Fig. 1 UV–Visible absorption of Au NPs formation with time

bands of absorption, (i) longitudinal absorption wavelength peak was more and (ii) transverse absorption wavelength peak was less. The strong function of NPs was reported to be the longitudinal plasmonic peak. Biomolecules interact explicitly with the NPs face through desorption and adsorption, the facial growth tariff is modulated kinetically, which ultimately controls the structure of NPs (Jo et al. (2016)). It is well known that the controlled metal salts reduction mediated with biomolecules typically favors in the development of spherical shaped NPs (Mohamad et al. 2013).

TEM analysis was utilized to evaluate the size distribution as well as the morphology of the fabricated Au NPs. HRTEM analyzed the morphology of the formed Au NPs as represented in Fig. 2a, b. TEM images also displayed that Au NPs are spherical shaped and have a smooth, non-aggregated surface where its size existed in the range of 40–50 nm. Results from previous literature also supported the TEM microscopic results of fabricated Au NPs in the current analysis (Vijayan et al. 2018). From the analysis of SAED patterns, we investigated the crystalline nature of formed Au NPs which displayed rings of bright diffraction spots (Fig. 2c). By these results, it is evident that the Au NPs formed using *Thuja occidentalis* plant extract are crystalline in nature. To evaluate the presence of crystal elemental Au NPs, we performed the Energy Dispersive Spectroscopy (EDS) study (Fig. 2d). A clear signal was noticed in the Au region on evaluation and it confirmed the fabrication of Au NPs. Also, the XRD analysis pattern of Au NPs displayed in Fig. 3 exhibited the presence of diffraction peaks of gold and corresponding diffraction peaks confirmed the face-centered cubic structure of prepared Au NPs.

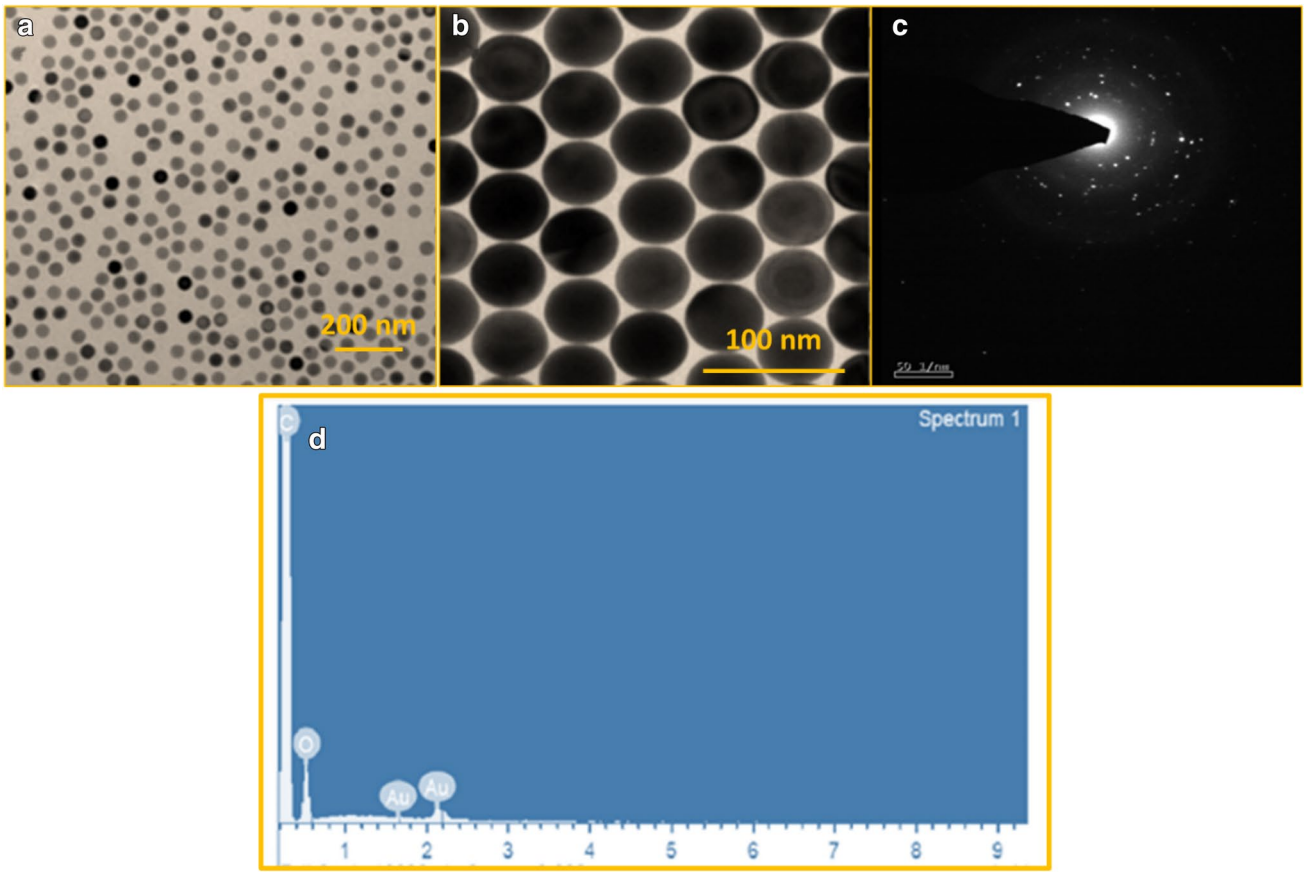

Fig. 2 HR-TEM images (**a, b**), SAED pattern (**c**) and EDS spectrum (**d**) of Au NPs

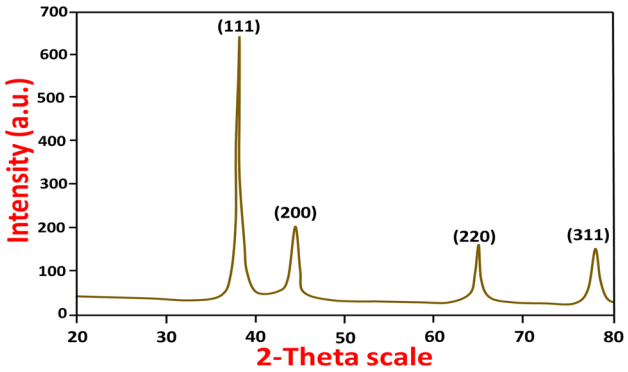

Fig. 3 XRD pattern of prepared Au NPs

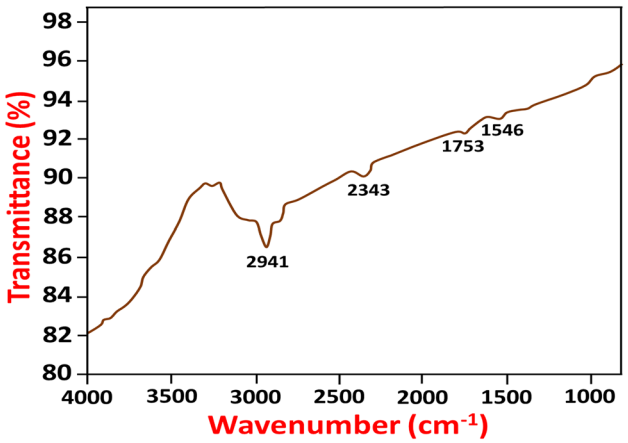

Fig. 4 FTIR spectra of prepared AuNPs

From the FTIR studies, we observed various peaks indicating the existence of active biomolecules on the Au NPs surface fabricated utilizing extracts of *Thuja occidentalis* (Fig. 4). The data from FTIR spectrum represented that various peaks of absorption were detected and located at 1546, 1753, 2373, and 2941 cm^{-1} range suggesting stretching vibrations of carboxylic acids and aldehyde groups of C–O–C, C–H, and O–H bonds. The bands of absorption found at 2373 and 2941 cm^{-1} range, corresponding to the C-H bond stretching vibrations of aromatic compounds. The bands identified at 1753–1556 cm^{-1}, suggests the existence of stretching vibrations of C–N (amines) and N–H present in the protein amide linkages. The spectrum of Au NPs from *Thuja occidentalis* extracts displayed strong resemblance, suggesting effective organic molecules adsorption on Au NPs.

In-vitro wound healing studies

Collagen synthesis at the incision region is a significant indicator of adhesion strength and wound adhesion. Immunocytochemistry displayed enhanced expression of collagen I of skin fibroblast subjected to Au NPs treatment. (Fig. 5).

The viability of skin fibroblasts presented in the skin after exposure to Au NPs is a prominent indicator for direct application on the incision site. Survival of skin fibroblast cells is decreased when they were exposed to Au NPs depending on the dose (Fig. 6). The MTT assay determined the IC_{50} value of Au NPs which was calculated to be 0.16 mg/mL (as shown in Fig. 7). On exposing fibroblast cells to Au NPs having 0.4 and 0.2 mg/mL concentrations has shown an obvious increase in the caspase 3 expression (Fig. 8).

We determined and compared the bacterial load from animals of daily administered Au NPs, single administered Au NPs as well as PBS administered at the incision site along with the line of the incision (Fig. 9). Significant reduction ($p < 0.05$) in the bacterial load percentage was found at the incision site of the rabbits administrated daily with Au NPs, when compared with the animals in the control group (15.3 ± 1.4 vs. 100; where n value is 4). On the other hand, the microbial load percentage at the operation site of animals with single-time treated Au NPs was not considerably different (where $p > 0.05$) from the animals in the control group (i.e. 94.9 ± 9.3 vs. 100; where n value is 4).

A crucial parameter reflecting healing response is time for complete wound healing. A considerable decrease

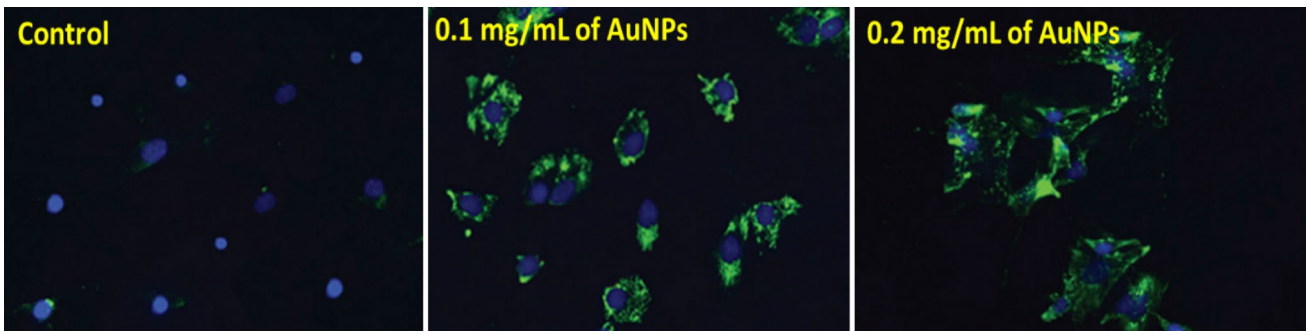

Fig. 5 Immunohistochemistry images showing the effect of Au NPs on collagen I expression from skin fibroblasts

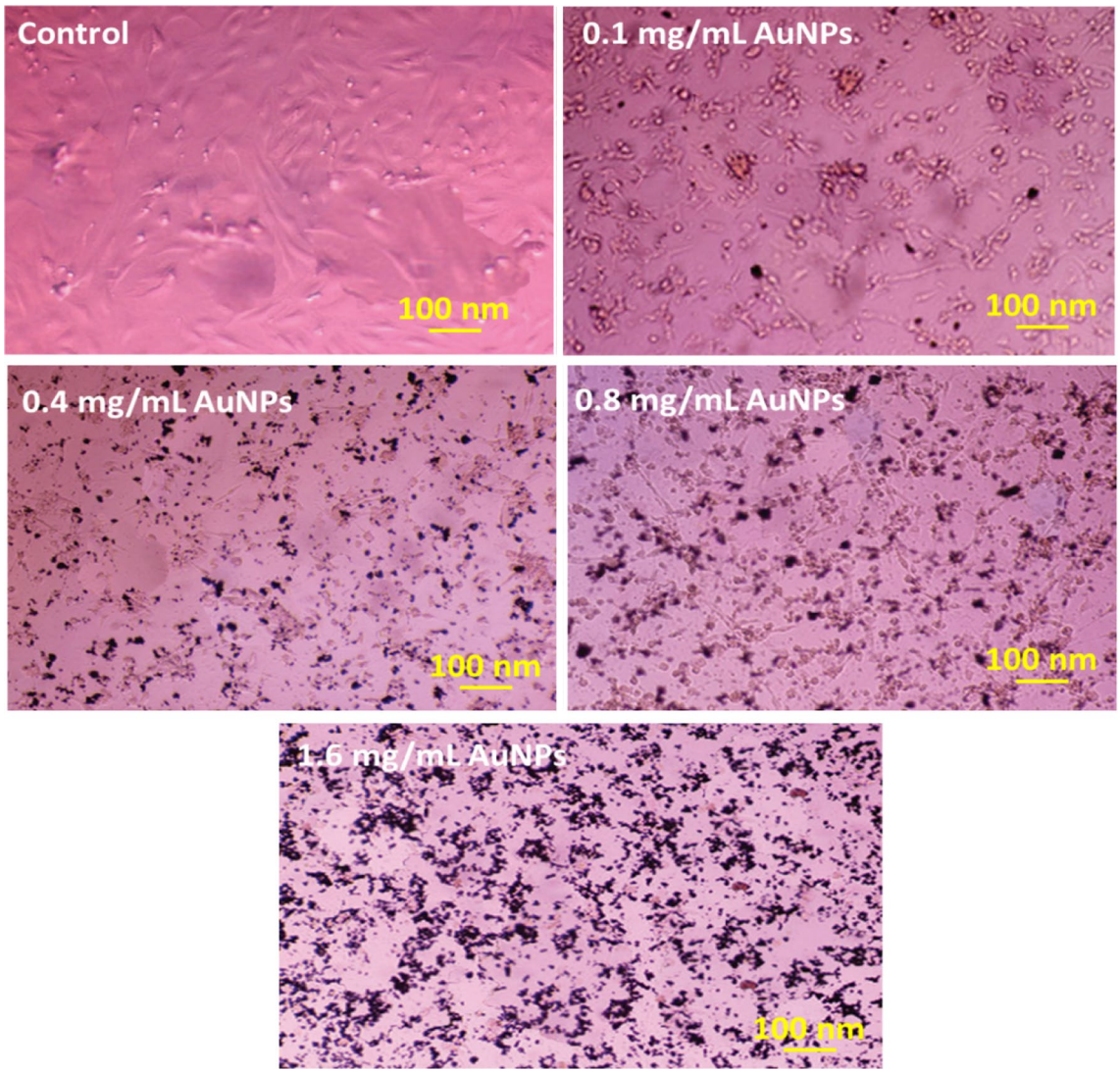

Fig. 6 Effect of Au NPs on survival of skin fibroblasts

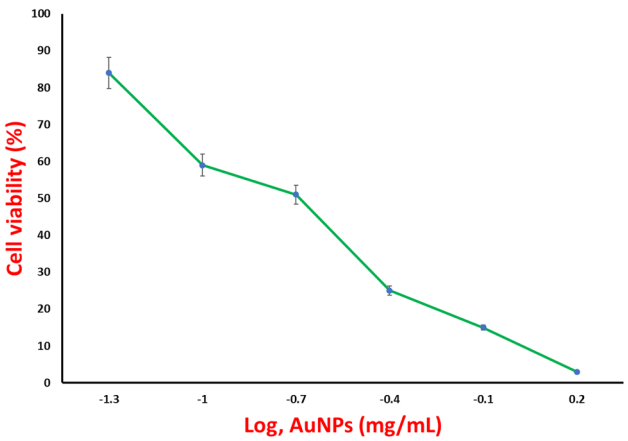

Fig. 7 Au NPs decline the skin fibroblast survival. Dose-dependent curves showing the cell viability post exposure with different doses of Au NPs

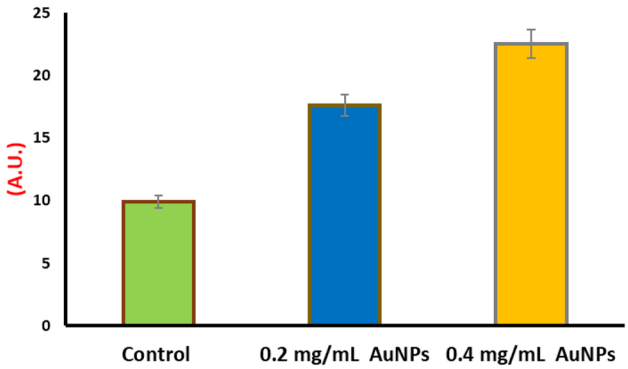

Fig. 8 Induction of caspase 3 in skin fibroblasts by Au NPs

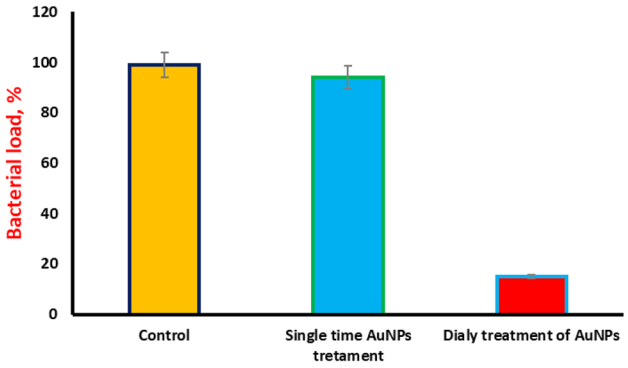

Fig. 9 Effect of Au NPs on bacterial load upon different treatments showed that Au NPs decreased the microbial load on the operational site

($p < 0.05$) in the time of wound healing was noticed in the daily AuNPs treatment group. The complete wound healing in animals treated daily with Au NPs is obtained within 3 days, while the average complete wound healing time in animals of the control group is found to be 5 days. On the other hand, complete wound healing was obtained on the 4th day in animals administrated with single-time treatment with Au NPs, which is not considerably different ($p > 0.05$) from the animals in the control group (Fig. 10). Therefore, the group of animals treated daily with AuNPs is noticed to have an enhancement in wound healing time.

For evaluating collagen deposition, the sections of histology from operation sites are stained using Sirius black. Sections of the operation site from animals administrated with AuNPs daily-demonstrated enhanced pink stained collagens with sirius red, when related with the control group animals. On the other hand, there was no substantial increase in the sections of animals treated with single AuNPs and was equivalent to the control group animals (Fig. 11).

These results exhibited an improved collagen appearance from skin fibroblasts upon treatment with AuNPs, which explained its use in wound healing applications. Noteworthy reduction in wound healing time was found subsequent exposure of AuNPs daily when related to single time treatment of AuNPs and control treatment, which is due to the improved deposition of collagen in the wound region as

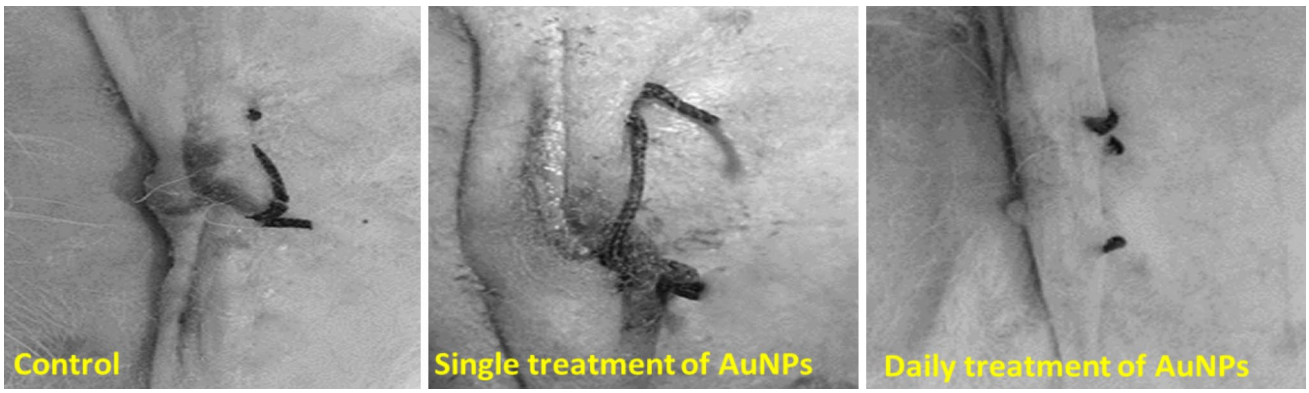

Fig. 10 Effect of Au NPs on early and improved wound healing with daily treatment of Au NPs. Photographic images of surgical site on 3rd day representing complete wound healing in animals treated daily with AuNPs, whereas incomplete healing in both control and animals treated with AuNPs single time

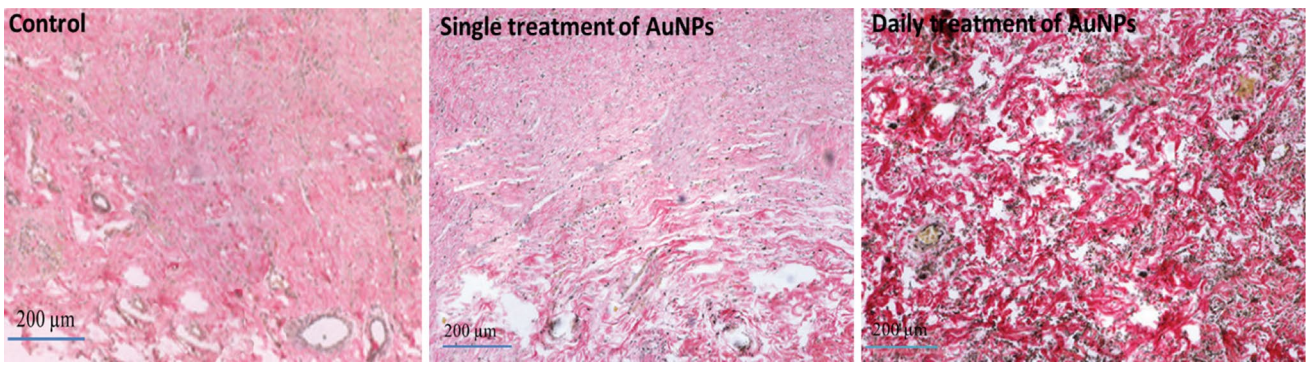

Fig. 11 Daily treatment of AuNPs improved collagen deposition on the surgical site. Sirius red staining displayed the improved collagen deposition in daily AuNPs treatments when related to control and single AuNPs treatment

observed by histological observations. These results also established the noteworthy decrease of microbial load at the surgical area upon the daily treatment of AuNPs, resulting in the fast-wound healing.

Conclusions

In conclusion, Au NPs were fabricated utilizing the *Thuja occidentalis* leaf extract. HR-TEM photographs confirmed the spherical shaped Au NPs of 40–50 nm particle size. Wound healing studies showed that Au NPs raised collagen production from dermal fibroblasts and higher treatment time improved the expression of caspase 3 and developed IC_{50} at 0.16 mg/mL concentration shows cytotoxic impact. Regular exposure to the surgical area led to a higher deposition of collagen, reduced microbial load, and enhanced healing of wounds.

References

Arhi C, El-Gaddal A (2013) Use of a silver dressing for management of an open abdominal wound complicated by an enterocutaneous fistula from hospital to community. J Wound Ostomy Continence Nurs 40:101–103

Chueh PJ, Liang RY, Lee YH, Zeng ZM, Chuang SM (2014) Differential cytotoxic effects of gold nanoparticles in different mammalian cell lines. J Hazard Mater 264:303–312

Geetha R, Ashokkumar T, Tamilselvan S, Govindaraju K, Sadiq MD, Singaravelu G (2013) Green synthesis of gold nanoparticles and their anticancer activity. Cancer Nano 4:91–98

Heller L, Levin S, Butler C (2006) Management of abdominal wound dehiscence using vacuum assisted closure in patients with compromised healing. Am J Surg 191:165–172

Hugh TB (1990) Abdominal wound dehiscence, editorial comment. Aust NZ J Surgery 60:153–155

Jo MR, Yu J, Kim HJ, Song JH, Kim KM, Oh JM, Choi SJ (2016) Titanium dioxide nanoparticle-biomolecule interactions influence oral absorption. Nanomaterials (Basel) 6:225

Koohi MK, Hejazy M, Asadi F, Asadian P (2011) Assessment of dermal exposure and histopathologic changes of different sized nanosilver in healthy adult rabbits. J Phys Conf Ser 304:012028

Kwan KH, Liu X, To MK, Yeung KW, Ho CM, Wong KK (2011) Modulation of collagen alignment by silver nanoparticles results in better mechanical properties in wound healing. Nanomed: Nanotechnol Biol Med 7:497–504

Liu HL, Dai SA, Fu KY, Hsu SH (2010) Antibacterial properties of silver nanoparticles in three different sizes and their nanocomposites with a new waterborne polyurethane. Int J Nanomed 5:1017–1028

Mawalla B, Stephen EM, Phillipo LC, Can I, William M (2011) Predictors of surgical site infections among patients undergoing major surgery at Bugando Medical Centre in Northwestern Tanzania. BMC Surgery 11:21

Mohamad NAN, Arham NA, Jai J, Had A (2013) Plant extract as reducing agent in synthesis of metallic nanoparticles: a review. AMR 832:350–355

Mokela JI, Kiviniemi H, Juvonen T, Laitinen S (1995) Factors influencing wound dehiscence after midline laparotomy. Am J Surg 170:387–390

Pal S, Tak YK, Song JM (2007) Does the antibacterial activity of Silver nanoparticles depend on the shape of the nanoparticle? A study of the gram-negative bacterium Escherichia coli. Appl Environ Microbiol 73:1712–1720

Spiliotis J, Tsiveriotis K, Datsis AD, Vaxevanidou A, Zacharis G, Giafis K, Kekelos S, Rogdakis A (2009) Wound dehiscence: is still a problem in the 21th century: a retrospective study. World J Emerg Surg 4:12

Vijayan R, Siby J, Beena M (2018) Indigofera tinctoria leaf extract mediated green synthesis of silver and gold nanoparticles and assessment of their anticancer, antimicrobial, antioxidant and catalytic properties. Artif Cells Nanomed Biotechnol 46:861–871

Publisher's Note Springer Nature remains neutral with regard to jurisdictional claims in published maps and institutional affiliations.